Seismic Analysis of Structures: Stress-resultant Interaction based on Response Spectra

Ana Rita Graça Tomaz
ana.rita.tomaz@ist.utl.pt

Instituto Superior Técnico, Lisboa, Portugal

June 2017

Abstract

The focus of this paper is to explore a methodology that characterizes a structure response to seismic excitations more accurately and less conservative than the one currently suggested in design codes. Besides being an interesting theoretical problem it has clear applications in the design of columns subjected to a combination of an axial force with a single or two bending moments (which is a major application field of seismic analysis). Such procedure can lead to significant reductions of the necessary steel reinforcement ratios allowing a material economy without compromising the structure safety. Furthermore, the principle of establishing correlations of variables in each individual mode and constructing a final interaction surface can be applied in different contexts such as the design of combined footings and equivalent static analysis.

Keywords: Seismic Analysis, Modal Combination Methods, Stress-resultant Interaction, Foundations, Equivalent Static Analysis

1. Introduction

The design of a reinforced concrete section relies on the evaluation of a set of variables, such as axial forces, bending moments or displacements.

These can be estimated by the response spectra method associated with a combination method for all the necessary individual linear analyses: for the n relevant modes and the $k = 3$ possible seismic directions. The most common combination methods are the ABS, the SRSS and the CQC ([1]).

The response spectra method provides the peak value for each of the variables. However, when more than one quantity is necessary for design, the widely used approach is to assume their most unfavorable combination. This can be overly conservative as the extreme values do not occur all at the same time.

The underlying idea is to properly consider the interactions between the stress-resultants in all the $n \times k$ structural analysis. This method can produce a surface in a x-dimension space that reproduces the interactions between the x variables, [2].

Afterwards this surface can be superimposed to the capacity curve of that section and optimize its design. We remark that the critical combination of a set of values on the interaction surface can not be determined without the knowledge of the resistant capacity surface. In fact, the critical combination does not necessarily include the maximum value of any of the variables, as it is the one closest to the capacity surface.

Gupta, [3], detailed the nature of the interaction surfaces constructed for a chosen set of design variables. It is proven that for 2 variables, as N and M in a column section, the result is an ellipse. For $n > 2$ this entity is a hyper-ellipsoid in a n-coordinate space where each point represents a set of simultaneous seismic response values. As the structures are also subjected to static loads the center of these elliptical envelopes must be shifted to include this effect. Finally, the interaction surface is completely defined and can be used for design. Being completely inscribed in a resistant capacity surface guarantees the section safety.

The work of Sessa, [4], follows this idea and focuses on calculating a parameter λ that multiplies each point of the interaction surface so that it becomes tangent to the capacity surface. If all the values λ are greater than the unity then the safety of the section is checked.

Some research has been done in order to simplify the security checks by choosing a set of points of the interaction surface and not the totality of them to be subjected to verification. In the work of Panetsos, [5], are studied four alternatives to chose the "most unfavorable" combinations of two variables (N and M), one being the simultaneity of maximum values. In Panetsos' study the differences in the reinforcement area can be as impressive as 54%,

which reiterates the importance of such investigations. A similar procedure is developed by [6] for combinations of 3 variables, which corresponds to a polyhedron in a 3D coordinate system that can have different shapes and number of vertices. Also in this paper is developed an equivalent static analysis as an alternative to the response spectra one.

This paper intends to explore the construction of interaction envelopes, using not only the method presented in [2] but also new ones that allow the display of the envelopes built with different mode combinations, see the companion dissertation [7] for further detail.

2. Theory

Without loss of generality let us consider just two variables (x_1, x_2), for example (M, N), whose maximum responses are calculated by the response spectra method and then combined. The two final values of these variables can be written as a vector $\boldsymbol{x_f} = [X_{f1}, X_{f2}]^T$ and represented in a coordinate space, see Figure 1. The classical envelope we would get is a rectangle constructed from the intersections of the straight lines defined by: $x_i = X_{fi}$ and $x_i = -X_{fi}$. As not all the points inside this rectangle reproduce a feasible response of the structure it should be reduced, see Figure 1.

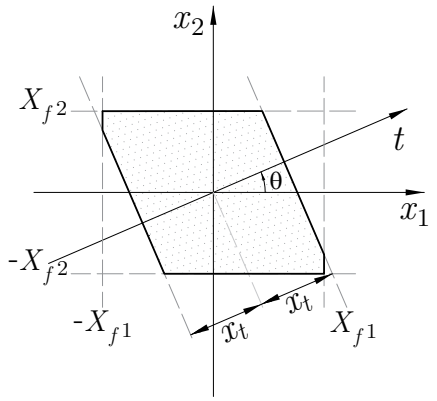

Figure 1: Rectangular and reduced envelope.

The starting point for this study has to be the analysis of each mode where there is a unequivocal relation between the stress-resultants. The information of each mode, i, is organized in a vector $\boldsymbol{x_i} = [x_{i1}, x_{i2}]^T$.

We also define the counterclockwise angle θ in the same coordinate space $(x_1 - x_2)$ and its vectorial representation $\boldsymbol{t} = [\cos\theta, \sin\theta]^T$.

Considering the projection of $\boldsymbol{x}$ on any vector $\boldsymbol{t}$ is introduced a distance x_t. For one mode x_{ti} and its square value are simply defined as:

$$x_{ti} = \boldsymbol{t}^T \boldsymbol{x_i} \tag{1}$$

$$x_{ti}{}^2 = \boldsymbol{t}^T \boldsymbol{x_i}\, \boldsymbol{t}^T \boldsymbol{x_i} = \boldsymbol{t}^T \boldsymbol{x_i}\, \boldsymbol{x_i}{}^T \boldsymbol{t} \tag{2}$$

Extending this to all the n relevant modes and adopting the SRSS combination one is led to:

$$x_t{}^2 = \sum_{i=1}^{n} x_{ti}{}^2 = \sum_{i=1}^{n} \boldsymbol{t}^T \boldsymbol{x_i}\, \boldsymbol{x_i}{}^T \boldsymbol{t} = \\ = \boldsymbol{t}^T \sum_{i=1}^{n} \left(\boldsymbol{x_i}\, \boldsymbol{x_i}{}^T\right) \boldsymbol{t} = \boldsymbol{t}^T \boldsymbol{X} \boldsymbol{t} \tag{3}$$

Here is introduced the interaction matrix, $\boldsymbol{X}$, which should to be adjusted to each combination method. For the SRSS combination, the definitions above directs us to:

$$\boldsymbol{X} = \sum_{i=1}^{n} \boldsymbol{x_i}\, \boldsymbol{x_i}{}^T = \begin{bmatrix} \sum_{i=1}^{n} x_{i1}{}^2 & \sum_{i=1}^{n} x_{i1} x_{i2} \\ \sum_{i=1}^{n} x_{i1} x_{i2} & \sum_{i=1}^{n} x_{i2}{}^2 \end{bmatrix} \tag{4}$$

On the other hand, for the CQC combination the definition of $x_t{}^2$ should be adapted to:

$$x_t{}^2 = \sum_{i=1}^{n} \sum_{j=1}^{n} \mu_{ij} x_{ti} x_{tj} \tag{5}$$

Causing the matrix $\boldsymbol{X}$ to be rewritten as:

$$\boldsymbol{X} = \sum_{i=1}^{n} \sum_{j=1}^{n} \mu_{ij}\, \boldsymbol{x_i}\, \boldsymbol{x_j}{}^T \tag{6}$$

With,

$$\mu_{ij} = \frac{8\xi^2(1+r)r^{(3/2)}}{(1-r^2)^2 + 4\xi^2 r(1+r)^2} \text{ and } r = \frac{p_j}{p_i} \tag{7}$$

The value x_t is the maximum distance any point of the envelope can take along the direction $\boldsymbol{t}$. This is why we can add two new straight lines to the set of lines that define the boundary of the interaction envelope. These new lines are perpendicular to $\boldsymbol{t}$ at a distance of x_t from the origin and will reduce the size of the original rectangular envelope, see Figure 1.

2.1. Intersection Method

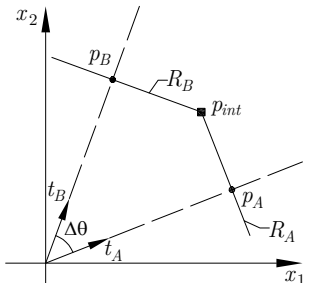

Figure 2: Interpretation of the intersection point, p_{int}.

Continuing the previous derivation, it should be noted that the point defined by $\boldsymbol{p} = x_t \times \boldsymbol{t}$ is not a point of the interaction envelope.

In fact, the point of the envelope can be any one belonging to the line perpendicular to $\boldsymbol{t}$ that contains $\boldsymbol{p}$, see Figure 2.

Taking two values of θ sufficiently close and their x_t, the envelope point is the intersection of the two perpendicular lines.

Defining Point A as: $\boldsymbol{p_A} = x_{tA}\boldsymbol{t_A}$, with $\boldsymbol{t_A}$ associated with a given θ_A and x_{tA} given by equation (5). The perpendicular line is: $R_A = x_{tA}\boldsymbol{t_A} + k_A\boldsymbol{n_A}$, where k_A is any real number and $\boldsymbol{n_A}$ as a realization of $\boldsymbol{n} = [-\sin\theta, \cos\theta]^T$.

Doing the same for Point B and matching the two perpendicular lines, the intersection point results in the following:

$$\begin{aligned} & x_{t_A}\boldsymbol{t_A} + k_A\boldsymbol{n_A} = x_{t_B}\boldsymbol{t_B} + k_B\boldsymbol{n_B} \\ & x_{t_A}\boldsymbol{t_A}^T\boldsymbol{t_B} + k_A\boldsymbol{n_A}^T\boldsymbol{t_B} = x_{t_B} + 0 \\ & k_A = \frac{x_{t_B} - x_{t_A}(\boldsymbol{t_A}^T\boldsymbol{t_B})}{\boldsymbol{n_A}^T\boldsymbol{t_B}} \\ & \boldsymbol{p_{int}} = x_{tA}\boldsymbol{t_A} + k_A\boldsymbol{n_A} \end{aligned} \tag{8}$$

By applying the same procedure to a range of θ values contained in $[0 - 2\pi]$, the shape of the envelope becomes apparent.

This method is directly applicable to the CQC and SRSS combinations by altering the matrix $\boldsymbol{X}$. Moreover, it is possible to adapt it for the ABS combination by changing the x_t definition:

$$x_t = \sum_{i=1}^{n} \left|\boldsymbol{t}^T\boldsymbol{x_i}\right| \tag{9}$$

Each graphic of Figure 3 displays a typical resultant envelope for the chosen combination and also the previous envelopes were drawn in gray to ease the comparison. (315 points were used, which corresponds to $\Delta\theta = 0.02$ rad.)

It is apparent that the resultant shape for the SRSS combination is elliptical with a significant correlation between the two variables, meaning that one of the semi-axis is significantly larger than the other.

The ABS envelope is a convex polygon exhibiting the same correlation which encloses SRSS envelope, showing it behaves as an upper bound to the other envelopes. It can be depicted as a group of pairs of parallel lines, each one introduced by one mode and whose length translates the mode relevance to the behavior of the structure. Even though the envelope could be constructed this way, it is more systematic to span the θ angles, calculate its x_t and use the intersection method.

Lastly, in this example the CQC envelope is so close to the SRSS solution that they overlap, meaning the modes have separated frequencies.

2.2. Extension to 3D

To approach the design of sections with bi-axial bending and axial forces, such as column in 3D structures, it would be simpler to apply a different method to construct the interaction surface.

The equation method assumes a elliptical shape for the envelope, proven by [2], and thus can only be used with a SRSS or CQC combination. The matrix $\boldsymbol{X}$ is still defined by equations (4) or (6), respectively.

The eigenvalues of these matrices are the square semi-axes of the resultant geometrical form called an ellipsoid. When ordered, they are labeled: a, b, and c. Using two angles α and β and making them vary in the respective ranges: $-\pi/2 < \alpha < \pi/2$ and $0 < \beta < 2\pi$, any point of the ellipsoid is defined in its principal axes by a vector $\boldsymbol{y}$:

$$\begin{cases} y_1 = a\cos(\alpha)\cos(\beta) \\ y_2 = b\cos(\alpha)\sin(\beta) \\ y_3 = c\sin(\alpha) \end{cases} \tag{10}$$

To write this vector $\boldsymbol{y}$ in the global coordinates,

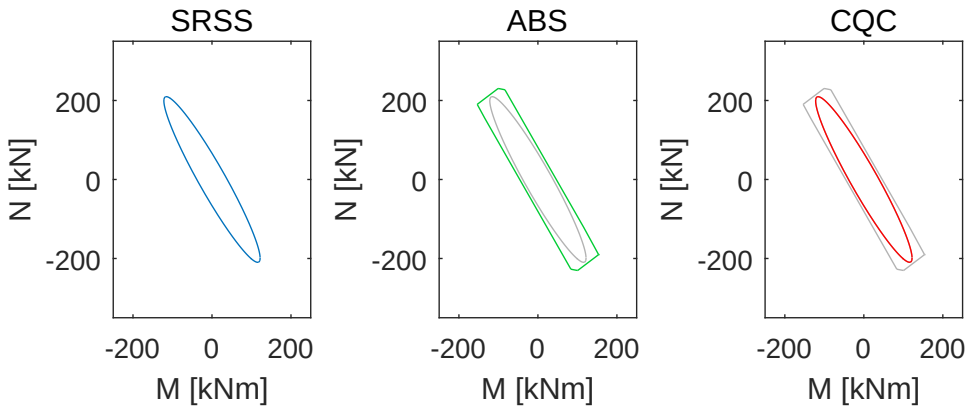

Figure 3: Perpendicular Method: SRSS, ABS, CQC.

we need to define the ellipsoid principal directions with the vectors: $\boldsymbol{v_i} = \sum_{k=1}^{3} V_{ki}\boldsymbol{e_k}$, which corresponds to the individual columns of the eigenvector matrix $\boldsymbol{V}$, see Figure 4.

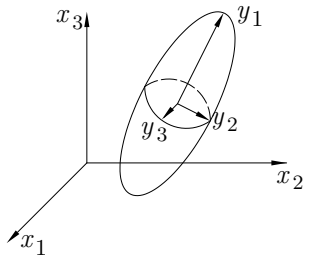

Figure 4: Two coordinate axis.

Finally, the vector $\boldsymbol{x}$ is obtained by:

$$\boldsymbol{x} = \sum_{i=1}^{3}\sum_{k=1}^{3} y_i V_{ki}\boldsymbol{e_k} \tag{11}$$

Doing this to an extensive number of combinations of the angles α and β materializes the 3D shape of the ellipsoid.

2.3. Safety Verification

To verify a section safety in a systematic way we begin by creating two vectors of points that describe the resistant and action curves in polar coordinates (r, θ), for each given value of N.

For the action envelope it is done by inverting the interaction matrix:

$$\boldsymbol{X}^{-1} = \left[\begin{array}{c|c} \boldsymbol{C_{MM}} & \boldsymbol{c_{MN}} \\ \hline \boldsymbol{c_{MN}}^T & C_{NN} \end{array}\right] \tag{12}$$

With these smaller matrices we can write the equation of the ellipses that result of the intersection of the ellipsoid with horizontal planes at given values of N:

$$(\boldsymbol{m}^T - \boldsymbol{m_0}^T)\frac{\boldsymbol{C_{MM}}}{{R_0}^2}(\boldsymbol{m} - \boldsymbol{m_0}) = 1 \tag{13}$$

With,

$$\begin{aligned} &\boldsymbol{m} = [M_2, M_3]^T \\ &\boldsymbol{m_0} = -\boldsymbol{C_{MM}^{-1}}\boldsymbol{c_{MN}}N \\ &{R_0}^2 = 1 - NC_{NN}N + \boldsymbol{m_0}^T\boldsymbol{C_{MM}}\boldsymbol{m_0} \end{aligned} \tag{14}$$

The resistant surface is also defined by an assembly of intersections with the same horizontal planes.

We divide the plane into sectors centered in each point of the resistant vector and analyze if any of the action vector points are within that section. If so we compare all the action point radii in the sector with the radius of the resistant point.

Given the case that in all sectors, all action point radii are smaller than the resistant point radius, we can ensure the safety of the cross-section, Fig 5.

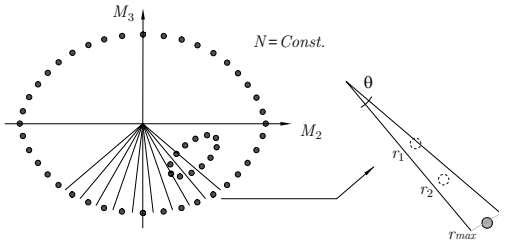

Figure 5: Safety verification mechanism.

Additionally, this verification can be done inside a cycle that increments the value of the total percentage of reinforcement, w_{tot}, allowing to find the optimized solution for the cross-section design. Note the increments do not need to be fixed and can be associated with a specific choice of commercials diameters for the steel bars.

3. Implementation

3.1. Seismic Definition

All the presented examples assume the same seismic action whose main parameters are in Table 1.

Table 1: Seismic Definition.

Earthquake	Zone	Ground	γ_I	q
Type 1	1.3	Type B	1	2.5

3.2. 2D Example

This example will address the design of the base section of the columns of a simple 2D structure, see Figure 6.

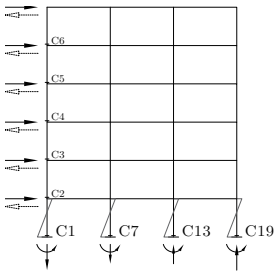

Figure 6: 2D Example.

The structure properties are summarized in the Table 2.

To resist the overturning moment of the seismic action (schematically represented as a horizontal force that can also have the other direction), the structure has two main mechanisms: bending moments in the fixed supports and a frame effect, ma-

Table 2: 2D Structure Description.

story height	span	concrete	steel
3 m	6 m	C30/37	A500
columns	beams	load	
0.3×0.3 m^2	0.3×0.6 m^2	34.5 kN/m	

terialized by axial forces with symmetrical signs in each pair of columns, see Figure 6.

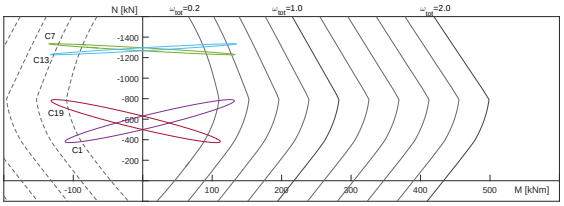

Figure 7: Action and resistant interaction curves.

As it can be seen in Figures 7 there is a substantial difference in the static values of N between interior and exterior columns. Additionally, the exterior ones have larger static M that slightly deviate the center of the envelopes. The seismic action produces a symmetric outcome between the left and right columns: the base sections have equal M combined with symmetric N to create a binary. This phenomenon is predominant in the outside columns which can draw larger values of N. The critical column is $C13$, requiring $\omega_{tot} = 0.5$.

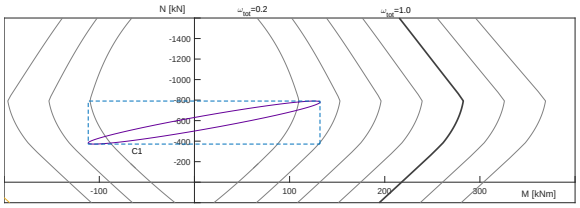

Figure 8: Comparison of envelopes for column $C1$.

Additionally, we should analyze column $C1$, isolated in Figure 8. In a dashed blue line is indicated the rectangular envelope commonly used for design. With this criteria would be necessary to design the section for $\omega_{tot} = 0.4$ ($A_s = 17$ cm^2). Conversely, using the interaction envelope $\omega_{tot} = 0.3$ would suffice. This corresponds to $A_s = 12$ cm^2 that can be materialized with $12\phi12$, allowing a saving of 25%.

3.3. 3D Example

The subject of the next study is a 3D structure that has an asymmetrical disposition of the columns, intended to correlate one earthquake direction to both bending moments, M_2 and M_3.

In addition to this there is a set of two close columns in each x alignment, see Figure 9. They will be used to design the combined footings.

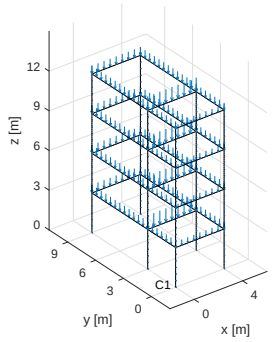

Figure 9: 3D example.

The same material and geometrical properties of the 2D structure were used, plus the ones indicated in Table 3.

Table 3: 3D Structure Description.

story height	span x	1$^{\text{st}}$ span y	2$^{\text{nd}}$ span y
3 m	4 m	3 m	6 m

To ease the visualization of the interaction ellipsoid, constructed for the base section of the column $C1$ with coordinates ($x = 0; y = 0$), its projections in the three coordinate planes are presented in Figure 10. We also present the individual responses for the earthquakes acting along the x and y directions. The $\boldsymbol{X}$ matrix, with dimension 3×3, is subdivided in smaller matrix with the two variables of the projection, for example:

$$\boldsymbol{P_{M_3 N}} = \begin{bmatrix} {M_3}^2 & M_3 N \\ M_3 N & N^2 \end{bmatrix} \tag{15}$$

These ellipses are defined by the following:

$$\boldsymbol{x}^T \boldsymbol{P}^{-1} \boldsymbol{x} = 1 \tag{16}$$

Where, $\boldsymbol{x} = [M_3, N]^T$ in this case.

Additionally, the x global axis is aligned with the e_2, in the elements referential, and the y with e_3.

As it can be seen, the direction X produces N and both moments, as the direction Y only produces N and M_2. Again this can be explained by the symmetry in the disposition of columns in one direction but not in the other.

For design purposes, we need to add the static stress-resultants, which will change the position of the ellipsoid center. With the correct placement, we can compare the action interaction ellipsoid with the resistant curves, using the safety verification method described in subsection 2.3. From it, we can conclude that the optimal total percentage of

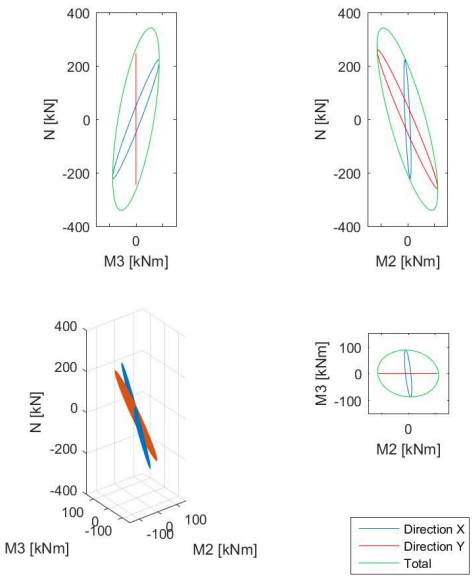

Figure 10: Ellipsoid projections (Column $C1$).

reinforcement is $\omega_{tot} = 0.7$. This correspond to $A_s = 29$ cm^2 that may be materialized with 16 ϕ16. Visually, it is clear in Figure 11 that this section verifies the safety criteria as the action curves are within the resistance curves for each value of the axial force, N, chosen to plot the curves.

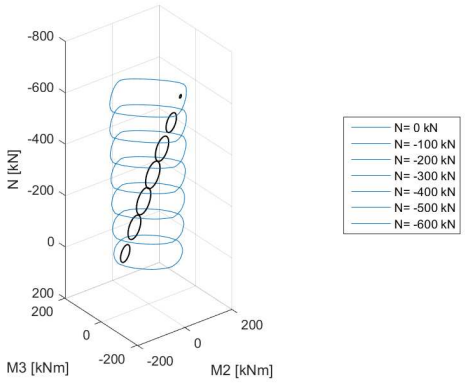

Figure 11: Action and Resistance for given values of N (Column $C1$).

4. Combined Footings

This is a particular design situation that arises when two columns are located sufficiently close to build a combined footing instead of two individual ones. The main reason to do so is the difficulty in verifying the safety to overturning due to column tension or large bending moments. The footing geometric dimensions are defined in Figure 12 and Table 4.

We begin with the stress-resultants in the base

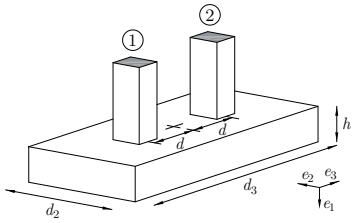

Figure 12: Combined footing.

Table 4: Footing characteristics.

σ_{max}	d_2	d_3	h	d
700 kPa	1.5 m	4.0 m	1.5 m	1.5 m

of each column for each mode, i, and earthquake direction, k.

$$N_{ik} = N_{1ik} + N_{2ik} + S_W \tag{17}$$

$$M3_{ik} = M3_{1ik} + M3_{2ik} \tag{18}$$

$$M2_{ik} = M2_{1ik} + M2_{2ik} - N_{1ik} \times d + N_{2ik} \times d \tag{19}$$

To correctly evaluate the axial force N_{ik}, the footing self-weight, S_W must be included.

The next stages are similar to what is done for a single section, assembling a matrix $\boldsymbol{X}$ with the stress-resultants correlated after the modes and directions are combined.

To evaluate the resistance of the footing, we adopt a plastic response of the soil, according to which the stress in the soil can only be null or equal to the maximum value, $\sigma = 0$ or $\sigma = \sigma_{max}$, in [kN/m^2].

Starting with a 2D analysis, Figure 13 displays the interaction ellipsoid, the components of its center and two dotted lines that represent the design criteria: one limits the soil stress to σ_{max} and the other limits the eccentricity so it is within the footing. The second behaves as an asymptote of the first.

For further detail we can analyze the foundation in 3D, calculating the resistance with a numerical method. In Figure 14 are plotted the action ellipsoid and the resistant surface, intersected at given values of N.

5. Equivalent Static Analysis

5.1. The 2D case

The idea behind a static equivalent analysis is to be able to calculate stress-resultants or displacements that are not exact but can reproduce the structures general behavior, with the upside of simplifying the calculations. This simplification comes from concentrating all the seismic information in a set of equivalent forces instead of constructing correlation matrices, X, for each studied section of the struc-

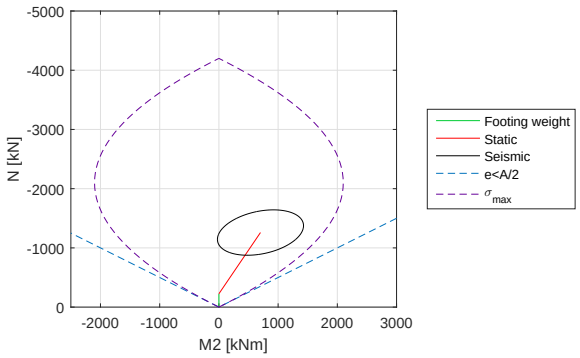

Figure 13: Safety Verification for the combined footing.

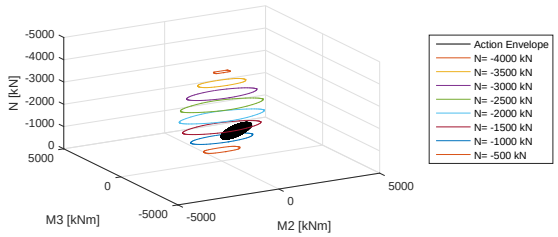

Figure 14: 3D Action and resistant interaction surfaces.

ture. The simplest way to accomplish a static analysis is to apply horizontal forces at the level of each floor, so the question becomes how to determine those forces.

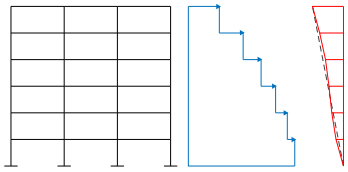

Figure 15: Shear Forces - Combined V.

Resorting to the 2D example, a possible approach is to sum the shear forces of the 4 columns of the same floor for each vibration mode and then combine them with a CQC combination. Between each floor, the shear forces have a constant value, which are plotted in blue in Figure 15.

The differences of the shear forces between floors can be understood as the equivalent static forces that simulate the seismic action. These forces in red follow the typical inverted triangle, in gray.

A different approach to estimating the equivalent forces is to start by calculating forces (differences of sequential shear values) in every mode and only after combining them with the CQC combination. This will be called the Combined F version.

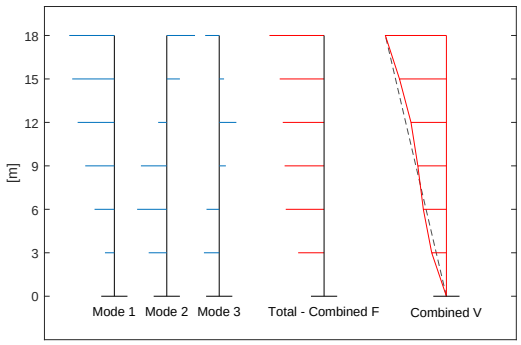

Figure 16: Equivalent forces in each mode and totals for the Combined F and Combined V.

Figure 16 shows the resulting forces in each mode and the total ones. The shape of each mode is apparent: with zero, one and two inflection points, respectively. Additionally, the final forces have an evolution in height similar to the Combined V version.

To a more appropriate comparison of the two methods, the final values of the equivalent forces are grouped in Table 5.

Table 5: Equivalent Static Forces.

Floor	Combined V	Combined F
6	93.78 kN	93.78 kN
5	72.06 kN	76.16 kN
4	54.37 kN	70.92 kN
3	43.86 kN	67.73 kN
2	35.43 kN	65.79 kN
1	22.58 kN	44.50 kN
$\sum$	322.08 kN	418.58 kN

Note the Combined F originates larger equivalent forces in every floor except the last were both methods correctly apply a force equal to the total shear force on that floor.

Furthermore, one evaluates the Base Shear: the combination of the shear forces acting on the base level of the structure in each mode. This quantity does not depend on any sequence of calculations and takes the value of 322.09 kN. This shows the Combined V provides a more accurate description of the structure response.

Figure 17 shows the stress-resultants $(M - N)$ in the base section of the columns in the alignment of $C1$ for the two static analysis (Combined V and Combined F) and the envelopes previously constructed with a dynamic analysis.

It is clear that the analyses show the same correlations of stress-resultants and that the Combined

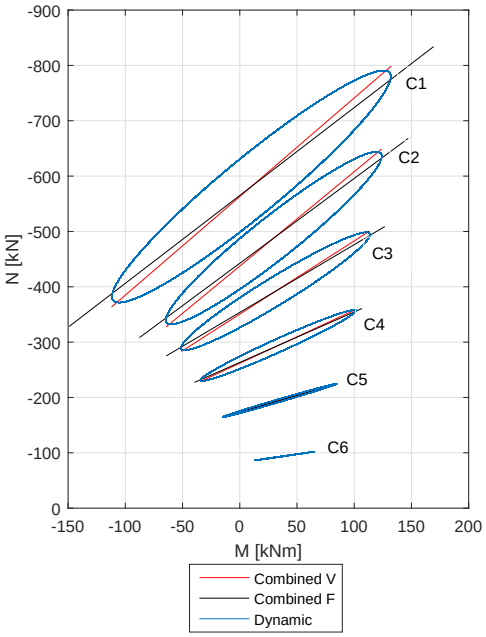

Figure 17: Comparison of stress-resultants from static and dynamic analysis.

V has a better fit to the major axis of the ellipse. It should be noted that the equivalent static result exceeds the envelope along the principal axis but, of course, underestimates the response perpendicular to it (a line can not reproduce an ellipse). This may aggravate the design of the section, depending on the positioning over the capacity surface.

5.2. The 3D case

The extrapolation of these methods to calculate equivalent forces in a 3D structure is not immediate and we will fully detail it.

To recreate each of the earthquake directions, the 3D structure has to be loaded with forces in the two directions x and y plus a torsional moment, at each floor.

At the level of each floor, and for each vibration mode, the total forces and moments are calculated by adding the contributions of each column, i, of that floor. The referential is in Figure 18.

$$\begin{aligned} V_x &= \sum_{i=1}^{n\ columns} V_{xi} \\ V_y &= \sum_{i=1}^{n\ columns} V_{yi} \\ {M_t}^V &= \sum_{i=1}^{n\ columns} (M_{ti} - V_{xi}y_i + V_{yi}x_i) \end{aligned} \tag{20}$$

Where x_i and y_i are the columns coordinates in any given referential. Afterward, these values are combined with the CQC combination.

Finally, for each floor, k, is created a correlation matrix $\boldsymbol{X}$, with the variables V_x, V_y and M_t^V. Note that these matrices have the same physical meaning to the ones used to define the interaction envelopes in terms of M_2, M_3 and N.

$$\boldsymbol{X_k} = \begin{bmatrix} {V_x}^2 & V_xV_y & V_xM_t \\ V_xV_y & {V_y}^2 & V_yM_t \\ V_xM_t & V_yM_t & {M_t}^{V\,2} \end{bmatrix} \tag{21}$$

These matrices have a graphic representation determined by the same procedure detailed above. These geometric figures are also ellipsoids and each point over that surface is a trio $[V_x, V_y, {M_t}^V]$, developed at the floor k and caused by one seismic direction.

The principle of the equivalent static forces is to choose one of these trios to represent the entire seismic action. For the orientation of the earthquake applied, in this case it is the direction x, we plot the ellipsoid and determine the point with the maximum value of V_x, see Figure 18. For an earthquake acting along the direction y is searched the point with the maximum V_y.

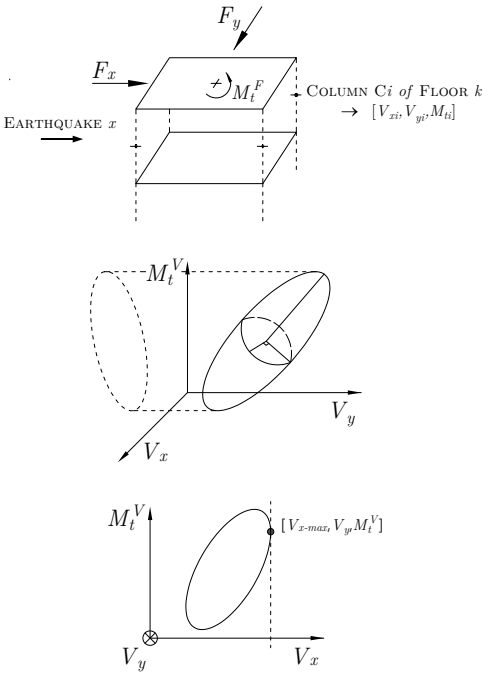

Figure 18: Trio of Equivalent Forces.

Obtaining the trios for each floor, and calculating the differences between them generates a set of equivalent forces $[F_x, F_y, {M_t}^F]$ that simulate the effect of each earthquake direction.

Note this follows the principle of the Combined V method used in 2D because it is the least conservative one.

The two sets of equivalent forces are then applied to the structure and two separate static analyses are performed. We remark that until this phase it is not relevant which sections of the structure we want to detail.

The values M_2, M_3 and N calculated for the desired section are gathered in the vectors $\boldsymbol{p_x}$ and $\boldsymbol{p_y}$. For each seismic direction, the possible combinations of stress-resultants are the ones over the lines that join the point defined by p to its symmetric.

We remark that is still necessary to combine the two earthquake directions to obtain an equivalent for the total interaction ellipsoid. The resultant equivalent surface is an ellipse, constructed with the intersection method and applying the principles of the SRSS combination of directions. Note the ellipse is contained in the inclined planed defined by the two directions, see Figure 19.

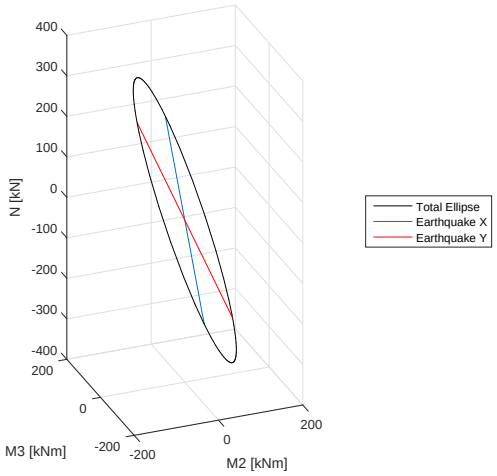

Figure 19: Equivalent Static Ellipse.

The maximum value N of the ellipse is 368.2 kN larger than the ellipsoid correspondent, which is 341.2 kN. This shows that along the plane that contains the ellipse it does behave as an upper bound to the ellipsoid.

In the same manner of the 2D static analysis, where the equivalent lines underestimate the ellipses behavior along their minor axis, so does this ellipse when compared to the ellipsoid. The reason it can be used to approximate the real behavior of the structure is because the ellipsoid does have one principal axis significantly smaller than the other two: the one perpendicular to the ellipses plane. See this values in Table 6.

Table 6: Ellipsoid and Ellipse semi-axes.

Semi-axis	Ellipsoid	Ellipse
1	357.94	359.46
2	93.96	86.61
3	19.76	0

6. Conclusions

To support the use of these interaction surfaces we remark that it resorts to the information typically calculated in seismic analysis, based on modal combinations and response spectra. The increase of computational effort to process that information is compensated by the material savings it allows in the design phase, by being less conservative to describe the effects of the seismic action. Such savings are described by specialized literature and reconfirmed in this dissertation.

Three different methods to construct the interaction envelopes were studied: the intersection, the divider and the equation method. Although all methods present the same outcome when is used an SRSS or CQC modal combination (which as an ellipse), only the intersection method can describe the ABS combination. This allowed the comparison of these three modal combinations, not just when applied to one variable but to combinations of two variables (such as $M - N$). As a result, we produced graphical representations of these common combinations in 2D.

When the study was extrapolated to 3D structures strategies to interpret the geometry of the interaction envelopes were developed. With a CQC modal combination, the interaction envelope is an ellipsoid. One strategy presented the projections of this 3D form in the three coordinate planes and the other intersected it with horizontal planes at different heights. Following this idea were constructed resistant capacity surfaces of the reinforced concrete sections also intersected at given values of the vertical coordinate, the axial force N. Having the action and resistant interaction surfaces, intersected by the same set of horizontal planes and overlapped in the same 3D plot, allows a visual design of the section. Additionally, we developed a procedure to automatically calculate the necessary steel ratio of a list of desired sections: the top and base sections on columns.

Taking the concept of correlating variables instead of designing with the maximum values of each, we applied it to a less common situation: combined footings. In this case, the interaction exists between the stress-resultants of the two columns that share the same footing. Using the modal information we developed mechanisms to quantify the action envelope and also the resistant capacity surface, once

again to allow its design.

Lastly, we approached an alternative to the construction of interaction surfaces, which implies calculating an interaction matrix and its graphic representation for each individual section. The idea is based on calculating a set of static forces equivalent to the seismic action that is applied once to the structure and originates the design stress-resultants in every desired section. This is developed for both 2D and 3D structures, having the shear forces as the starting point to calculate the equivalent static forces.

The 3D case is more complex as it involves two shear forces and a torsional moment. The calculation of the equivalent forces also resorts to the concept of interaction surfaces of these stress-resultants and to the selection of one of those points. The final output, once the equivalent static forces are applied, is an ellipse in a 3D coordinate space which approximates the complete interaction ellipsoid.

These concepts were exemplified with simple and regular structures reason why the domains of validity of these static analyses need further study.

Acknowledgements
The author would like to thank her supervisors Prof. Manuel Corrêa and Prof. Luís Guerreiro for their guidance and endless dedication during the development of this work and also her family and friends for company and support.

References

[1] A. Der Kiureghian. Structural response to stationary excitation. *Journal of the Engineering Mechanics Division*, 106(6):1195–1213, 1980.

[2] C. Menun and A. Der Kiureghian. Envelopes for seismic response vectors. I: Theory. *Journal of Structural Engineering*, 126(4):467–473, 2000.

[3] A.K. Gupta and M.P. Singh. Design of column sections subjected to three components of earthquake. *Nuclear Engineering and Design*, 41(1):129–133, 1977.

[4] S. Sessa, F. Marmo, and L. Rosati. Effective use of seismic response envelopes for reinforced concrete structures. *Earthquake Engineering & Structural Dynamics*, 44(14):2401–2423, 2015.

[5] P. Panetsos and K. Anastassiadis. Evaluation of the most unfavorable combinations of simultaneous element forces, for the design of R/C cross section subjected to isotropic seismic excitation. In *Proceedings of the eleventh European Conference on Earthquake Engineering*. AA Balkema, 1998.

[6] S. Erlicher, Q.Q. Nguyen, and F. Martin. Seismic design by the response spectrum method: A new interpretation of elliptical response envelopes and a novel equivalent static method based on probable linear combinations of modes. *Nuclear Engineering and Design*, 276:277–294, 2014.

[7] A.R. Tomaz. Seismic analysis of structures: Stress-resultant interaction based on response spectra. Master's thesis, Instituto Superior Tcnico, 2017.